https://doi.org/10.1595/205651318X15318154729616 *Johnson Matthey Technol. Rev.*, 2018, **62**, (4), 407–416

JOHNSON MATTHEY
TECHNOLOGY REVIEW

www.technology.matthey.com

Using Catalytic Heat Recovery to Improve Efficiency of Gasoline Spark Ignition Engines

Chemical efficiency calculations predict fuel economy improvements up to 14%

By Perry Leung, Athanasios Tsolakis*, José M. Herreros, Miroslaw L. Wyszynski
Mechanical Engineering, University of Birmingham, Birmingham B15 2TT, UK

Stan E. Golunski
Cardiff Catalysis Institute, School of Chemistry, Cardiff University, Cardiff CF10 3AT, UK

***Email:** a.tsolakis@bham.ac.uk

Exhaust gas recirculation is a widely used technology on conventional vehicles, primarily for lowering emissions of local pollutants. Here we use chemical models to show that an exhaust-gas recirculation loop can be converted into a heat-recovery system by incorporating a catalytic reformer. The system is predicted to be particularly effective for gasoline-fuelled spark ignition engines. The high temperature and low oxygen-content of the exhaust gas mean that endothermic reactions will predominate, when some of the gasoline is injected into the recirculation loop upstream of the reformer. The output of the reformer will, therefore, have a higher fuel heating value than the gasoline consumed. Chemical efficiency calculations, based on the predicted reformer output at chemical equilibrium, indicate that the direct improvement in fuel economy could be as high as 14%. Initial tests using a rhodium reforming catalyst suggest that much of the heat recovery predicted by the thermodynamic models can be achieved in practice, which together with a reduction in throttling may allow a gasoline spark ignition engine to match the fuel economy of a diesel engine.

Introduction

The 2014 Intergovernmental Panel on Climate Change attributed about 14% of total green house gas (GHG) emissions to transportation (1). Carbon dioxide is the most significant, accounting for 80% of global GHG emissions, with the road fleet of vehicles responsible for about 20% of all anthropogenic emissions (2). A major proportion of the CO_2 arises from the inherent inefficiency of the internal combustion engine, which radiates heat, requires cooling and braking, and releases hot exhaust gas into the atmosphere. Each of these sources of inefficiency is currently being addressed in the universal push towards higher fuel economy and lower CO_2 and pollutant emissions. Among the most challenging is the recovery of waste heat from the exhaust, with the organic Rankine cycle (3), electric turbocompounding (4) and thermoelectric (5) technologies being most commonly under investigation (6). However, another technology – which provides a chemical route to heat recovery – is emerging as a serious contender. This is exhaust gas reforming, in which some of the primary fuel is injected into a catalytic reactor fitted inside an exhaust gas recirculation loop (7, 8). The catalyst enables the fuel to react with the oxygen, water and CO_2 in the stream of exhaust gas to produce reformate (mainly carbon monoxide, hydrogen and nitrogen), which is fed back to the engine. Providing the reactions taking place in the reformer are net endothermic, the process will have the combined and interrelated effects of recovering heat, increasing the heating value of the fuel, improving fuel economy (7) and lowering CO_2 and the other regulated gaseous and particle emissions (8).

The gasoline (petrol) spark ignition (SI) engine is a particularly suitable candidate for this approach to heat recovery. The low O_2 content of the exhaust gas means that exothermic oxidation reactions can only play a minor role in the reformer. On the other hand, the consistent supply of steam and CO_2 provides the coreactants for the endothermic routes to CO and H_2 production. During stoichiometric or near-stoichiometric SI combustion, the exhaust-gas temperatures are usually in the range of 550–700°C, but can be as high as 950°C near the exhaust port (particularly at high engine loads). At these temperatures (550–950°C), the conversion of gasoline to reformate would not be expected to be substantially limited either by the chemical equilibria or by the kinetics of the endothermic reactions, unlike the situation for diesel combustion, where the exhaust-gas temperatures are much lower.

The catalyst technology for exhaust gas reforming owes much to three-way catalysis (9) and to the autothermal reforming process known as HotSpot™ (10, 11) which had been developed as a means of on-board hydrogen generation for fuel cell powered vehicles (12–14). The earlier work highlighted that rhodium (in the form of supported nanoparticles) is one of the most effective reforming catalysts under exhaust gas conditions. It has since been shown to be capable of converting a broad range of fuel molecules (including methane (15), ethanol (16), propane (17) and *iso*-octane (18)) into a hydrogen-rich product stream. Apart from its ability to catalyse the key fuel-reforming reactions (shown in the section Method and Experimental Setup), supported rhodium can resist the deactivation often caused by the large temperature excursions and carbon-depositing reactants that can prevail in vehicle exhausts.

In this study, we examine the practical feasibility and potential benefits of exhaust gas reforming for heat recovery on board gasoline-fuelled vehicles for a wide range of engine operating conditions. Based on chemical equilibrium models, we have predicted the likely composition of the reformate produced as a function of temperature, for two conceptual system designs. We have then tested whether these reformate compositions can be achieved in practice in a range of realistic vehicle operating conditions, before estimating the impact on fuel economy. Additionally, this work provides new knowledge to guide the control of on-board fuel reforming, as well as on the usefulness and limitations of simple thermodynamic models (for example, based on reaction stoichiometry or chemical equilibrium) which could be integrated into real-time vehicle control models.

Method and Experimental Setup

Engine-Reformer Models

A key requirement of an exhaust gas reformer is its ability to maintain high chemical efficiency over a broad range of engine conditions which result in different exhaust gas flow rates, compositions and temperatures. During the lifetime of a passenger car, the majority of the fuel used, and thus CO_2 produced, is at engine speeds below 3000 rpm. **Figure 1** shows the typical torque range measured for a multicylinder gasoline fuelled vehicle. For the reforming technology to find application, therefore, it has to be most efficient at operating points that lie within the speed-torque window shown in the figure. Specific engine speed-torque conditions will be different depending on the engine characteristics as well as on the vehicle and its driving cycle. Thus, representative engine speed-torque conditions were selected within this operating area, which covers conditions derived from several driving cycles. This allowed us to study the effects of realistic exhaust temperature, residence time and composition upstream of the reformer on potential fuel savings when the reforming process is coupled with the engine. At higher engine speeds (>3000 rpm), the engine exhaust is hotter and the reforming efficiency is expected to be improved, as long as the process does not become mass-transfer and/or kinetically limited due to the increased space velocities of the reactants through the catalyst bed of the reformer.

The exhaust gas temperature (T_{ex}) operating window for all engine points was 425–700°C (**Figure 1**, **Table I**). The final temperature range selected for the engine-reformer models was extended to 900°C to include expected temperatures at higher loads. Exhaust gas composition does not vary greatly for an SI engine operating at lambda ~1 (the typical combustion stoichiometry for a gasoline engine), thus we were able to reduce the number of independent parameters by assuming that the component concentrations would be constant, by calculating the average of all operating conditions (O_2 = 1.3%, CO_2 = 13.86%, CO = 1.02%, H_2O = 12% and N_2 = 71.82%). Although the addition of reformate to the engine will alter to some extent the composition (8) and temperature of the exhaust gas, these effects were not considered in this study. In order

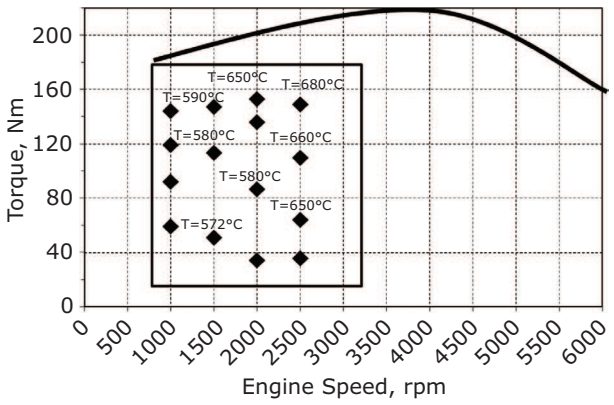

Fig. 1. Typical multicylinder engine speed-torque window, showing the individual operating points used as inputs in the system models. The curved boundary represents the peak torque value as function of engine speed

to simulate the effect of different space velocities of the reactants through the catalyst, two different engine-reformer systems were modelled:

- In System 1, a mode of operation was simulated in which the flow rate of exhaust gas to the reformer (**Table I**, last column) can be altered depending on the engine operating condition, and thus the gas hourly space velocity (GHSV) through the reformer also changes. Therefore, the fuel feed-rate to the reformer has to be adjusted to maintain the inlet ratios at O_2:C = 0.5, H_2O:C = 1 and CO_2:C = 1 for optimum CO and H_2 production, and for maximum heat recovery.
- In System 2, the flow rate of exhaust gas to the reformer is fixed (at the minimum value shown in **Table I**). In this case, the fuel feed-rate is also constant (i.e. exhaust gas flow rate = 224 l min^{-1}, fuel feed-rate = 4.8 g min^{-1}). The main advantage of this system is its simplicity, arising from the fixed reactant ratio used to feed the reformer. The only parameter that is changing in the model is the exhaust gas temperature.

Calculations based on reaction stoichiometries were used to predict the maximum theoretical efficiency of both systems. It was assumed that the gasoline (with an empirical formula of $C_{6.4}H_{11.7}$), when added to the reformer, is completely converted by reaction with all the available O_2, H_2O and CO_2 in the exhaust gas recirculation loop, through the three major reforming reactions (Equations (i)–(iii)):

Dry reforming:

$$C_{6.4}H_{11.7} + 6.4CO_2 \rightarrow 12.8CO + 5.85H_2 \quad \Delta H = +1371 \text{ J mol}^{-1} \quad \text{(i)}$$

Steam reforming:

$$C_{6.4}H_{11.7} + 6.4H_2O \rightarrow 6.4CO + 12.25H_2 \quad \Delta H = +1252 \text{ J mol}^{-1} \quad \text{(ii)}$$

Partial oxidation:

$$C_{6.4}H_{11.7} + 3.2O_2 \rightarrow 6.4CO + 5.85H_2 \quad \Delta H = -564.5 \text{ J mol}^{-1} \quad \text{(iii)}$$

Table I Engine, Exhaust and Reformer Conditions for the Operating Points Used as Inputs in the System Models

Test	Engine operating conditions			Exhaust from engine					Reformer inputs	
	NMEP[a], bar	Speed, rpm	Air-flow, l min^{-1}	T_{ex}, °C	CO, %	CO_2, %	THC, ppm	O_2, %	Fuel, g min^{-1}	Exhaust gas, l min^{-1}
1	4.9	1010	810	492	1.30	13.60	160	1.78	4.8	224
2	3.5	1011	572	425	0.91	14.00	262	1.38	4.8	224
3	6.1	1010	1020	517	1.24	13.50	114	1.67	6.9	323
4	7.1	1010	1125	528	1.24	13.60	101	1.53	7.1	330
5	3.2	1515	808	495	1.77	13.70	234	1.31	5.3	249
6	6.2	1515	1192	554	0.91	13.90	173	1.28	8.0	373
7	7.8	1515	1366	581	1.01	13.80	135	1.32	10.9	511
8	2.5	2019	864	541	0.92	13.90	211	1.30	5.7	267
9	5.1	2019	1245	578	0.88	14.00	184	1.09	8.6	402
10	8.3	2019	1597	638	0.95	13.90	134	1.18	14.5	678
11	2.7	2523	1059	624	0.89	13.90	159	1.32	7.3	342
12	4.1	2523	1282	645	0.72	14.20	131	1.02	9.2	431
13	8.3	2523	1755	675	0.82	14.00	128	1.08	16.7	781

[a] Net mean effective pressure

The input power was calculated from the rate at which gasoline is fed to the reformer, and the output power from the rate at which the reformate (CO and H_2) is formed; the efficiency was calculated from the output:input power ratio. An efficiency value >100% indicates that: (a) the reactions in the reformer are net endothermic; (b) the reformate formed has a higher heating value than the gasoline consumed in the reformer; and (c) the reformer is functioning as a heat recovery unit.

In practice, whether the maximum theoretical efficiency can be achieved by the reformer will be determined by both thermodynamics (the chemical equilibria established in the reactor) and kinetics (the rate of catalytic activity). To achieve the next predictive level in our system models (thermodynamic feasibility), a chemical equilibrium solver (STANJAN) was used to establish the equilibrium composition of the reformer products, based on standard thermodynamic data (from US Department of Commerce, National Institute of Standards and Technology (NIST)-JANAF tables). The solver took into account the pressure, temperature and enthalpy of the reactants fed to the reformer (the exhaust gas components and the added fuel) at each of the chosen operating points for both system designs. Once again, the empirical formula ($C_{6.4}H_{11.7}$) and properties of the gasoline added to the reformer in the experimental study (see below) were used to represent the fuel in the calculations.

Engine-Reformer Experiments

Engine and Engine Instrumentation

In order to assess whether the efficiencies predicted from the thermodynamic calculations could be achieved in practice, a small-scale reforming reactor was fed with exhaust from a naturally-aspirated, single cylinder experimental engine (four-stroke; four valves per cylinder; spark-ignition; water cooled). Further specifications are provided in **Table II**. Although the exhaust gas composition (**Table III**) was not identical to that produced by the multicylinder engine (**Table I**), both engines emitted very similar concentrations of the key co-reactants (CO_2 and H_2O) required for the endothermic reforming of gasoline. An electric dynamometer was used to load and motor the engine. The engine test rig included instrumentation to allow all flows (fuel, intake air and exhaust gas), temperatures (oil, air, inlet and exhaust manifold) and pressures to be monitored. Atmospheric conditions (humidity, temperature, pressure) were also monitored during the tests.

Table II Engine Specifications

Item	Value
Bore × stroke, mm	90.0 × 88.9
Swept volume, cm^3	565.6
Compression ratio (geometric)	11.5:1
Fuel delivery	Port injection (3 bar) and direct injection
Valves	Intake/exhaust
Lift, mm	10.5/9.3

Small-Scale Reformer

The reforming tests were conducted in a small-scale reactor described in earlier publications (17). The reactor contained a ceramic monolith (900 cpsi; 22 mm diameter × 270 mm length) coated in a catalyst with a nominal composition of 1%Rh/CeO_2-ZrO_2 (by weight). The coated monolith was a proprietary formulation for autothermal reforming of hydrocarbons, supplied by Johnson

Table III Typical Exhaust Gas Composition and Resultant Reformer Test Conditions

Exhaust gas composition					
CO, %	**CO_2, %**	**O_2, %**	**H_2O, %**	**THC, ppm**	
0.28	13.1	2.4	12.48	5224	
Reforming conditions					
Temp.[a], °C	**Ex. gas[b], l min^{-1}**	**GHSV[c], hr^{-1}**	**O_2:C**	**S:C**	**Fuel flow[d], ml h^{-1}**
600–950	3	2000	0.07	0.69	37.2

[a] Temperature measured at the inlet of the monolith catalyst

[b] Engine exhaust gas flow rate to the reformer

[c] Gas hourly space velocity of the reactants

[d] Fuel flow rate to the reformer

Matthey, UK. The reactor was held vertically in a tubular furnace, which was heated to a pre-set temperature. The reactor inlet-temperature was measured by a K-type thermocouple located close to the front face of the monolith bed. The reactor inlet temperature was changed (by controlling the heating rate of the furnace) emulating the exhaust-gas inlet temperature of a full size system coupled to an engine. (In practice, the reformer would not be electrically heated.) A second thermocouple, placed inside the central cell of the monolith, could be used to record the axial temperature profile, by moving it along the length of the monolith channel. The reactor inlet-temperature was controlled over the range of 600–950°C. The lower limit was selected to ensure successful operation of the experimental testing by ensuring that all the fuel components were in the gas-phase before coming into contact with the catalyst, while the upper limit represented the maximum exhaust gas temperature expected at high engine loads. The fuel and reactant flow rates were chosen to replicate an experimental O_2:C ratio within the range of the modelling study. The O_2:C was low (high catalyst equivalence ratio) to mimic gasoline exhaust, which favours endothermic reforming reactions such as steam and dry reforming rather than complete and partial fuel oxidation.

A commercial gasoline fuel (provided by Shell Global Solutions, UK) was used throughout this study. The main fuel properties are listed in **Table IV**.

A medical syringe pump was used to feed the gasoline to a U-tube inside the tubular furnace (**Figure 2**), where it mixed with the exhaust from the single-cylinder engine. This ensured that the temperature of the fuel-enriched exhaust had thermally equilibrated before it reached the catalyst bed. The resultant conditions for the reforming tests are shown in **Table III**.

Analysis of Exhaust Gas and Reformate

A multiple analyser (MEXA 7100 DEGR, HORIBA, Japan) was used to measure CO, CO_2, O_2 and total

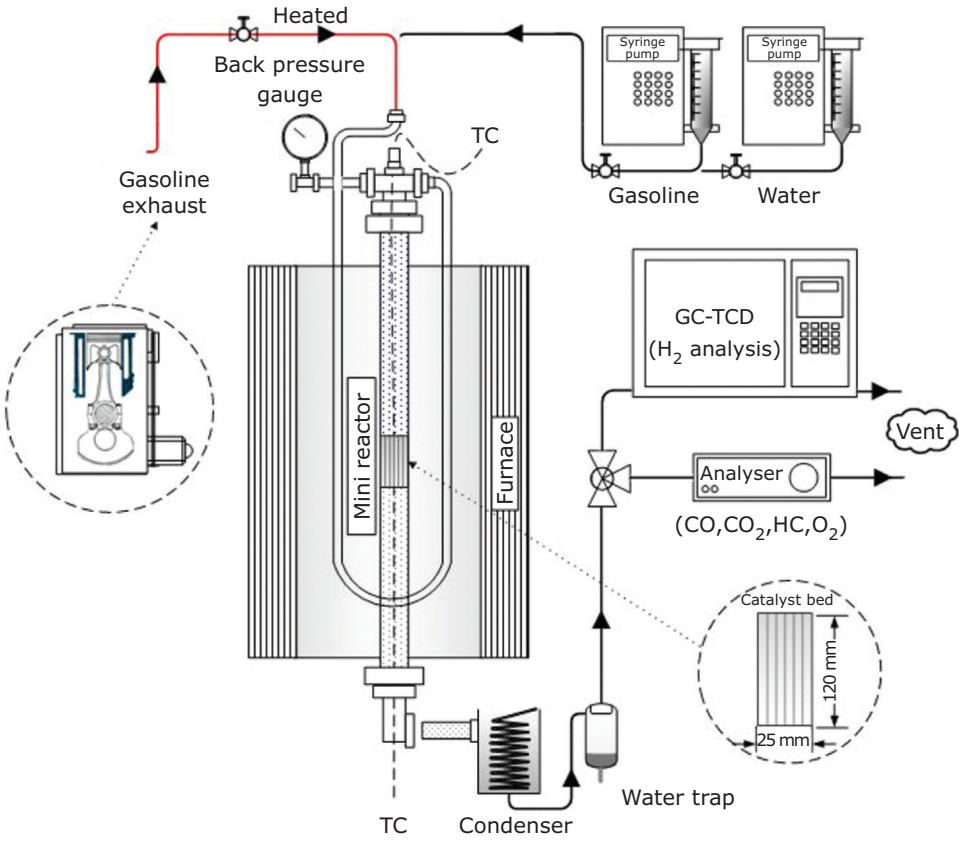

Fig. 2. Experimental arrangement for exhaust gas reforming tests, in which a small-scale reformer is fed with exhaust gas (from a single cylinder engine) to which gasoline is added. GC-TCD = gas chromatography-thermal conductivity detector

Table IV Fuel Properties	
Item	**Value**
Empirical formula	$C_{6.4}H_{11.7}$
Density @15°C, kg l^{-1}	0.7387
EN12:94, kPa	984
IBP, °C	28.6
10%	37.9
50%	93.4
90%	160.1
FBP	96.3
ASTM D2622-94, (WDXRF, A/43)	23
Net heating value, MJ kg^{-1}	43

hydrocarbon (THC) concentrations. Additionally, for detecting and measuring the H_2, a gas chromatograph (HP 5890, Hewlett Packard, USA) equipped with a thermal conductivity detector was used. It contained a double separation column: 1 m HayeSep® Q (80–100 mesh), followed by a molecular-sieve-coated capillary column Molesieve 5A (MS5A).

Results

Part I: Engine-Reformer Models

Predictions of Reformer Output

Equilibrium reformer outputs over the extended temperature range (450–900°C) for constant exhaust gas composition are depicted in **Figure 3**. Even at the lowest inlet temperature considered (450°C), the equilibrium calculations predict that all the oxygen and H_2O will be consumed. Although CO and H_2 will already be generated, the major components exiting the reformer are expected to be CO_2 and CH_4. In practice, the most likely mechanism for CH_4 formation would be by cracking of the higher-hydrocarbon components of the gasoline, or through methanation of CO by reaction with H_2. As the temperature rises, the equilibrium concentrations of both CO_2 and CH_4 are predicted to decline, while the concentrations of CO and H_2 will increase. As the temperature reaches 800°C, the calculations predict that the conversion of gasoline will approach 100%, resulting in the concentrations of CO and H_2 stabilising (at around 25% and 20% respectively) and the concentrations of product CO_2, H_2O and CH_4 becoming negligible. Over the temperature range of an average drive cycle, the equilibrium concentrations of the key reforming products (CO and H_2) are predicted to rise in tandem by about 10% in the exit stream.

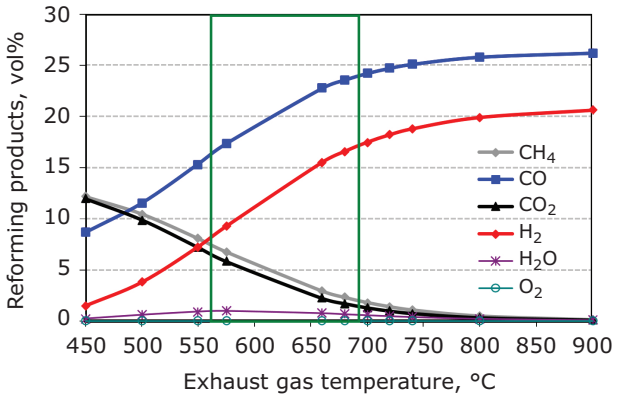

Fig. 3. Predicted composition of reformer product stream as a function of inlet temperature, at chemical equilibrium. Higlighted zone corresponds to the temperature range of the exhaust gas produced during an average drive cycle

Predictions of System Performance

For System 1 (variable exhaust and fuel flow rates through reformer) using the stoichiometric model, the chemical power delivered to the reformer is predicted to increase from 2.5 kW at the first operating point to 9.8 kW at the last operating point. The effect of the reformer is to raise the chemical power (by over 25%), through the endothermic reactions between the exhaust gas and the added fuel, across the complete range of conditions (**Figure 4**). For System 2 (fixed exhaust and fuel flow rates), the reformer is predicted to raise the power of the fuel by about 0.75 kW under all the modelled conditions. Both sets of calculations are based only on the heating values of the primary fuel consumed (injected upstream of the reformer) and the secondary fuel produced (H_2, CO and CH_4)

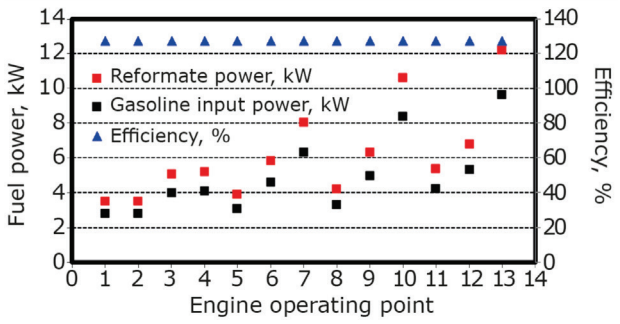

Fig. 4. Process efficiency and fuel power (kW) based on stoichiometric reactions

in the reformer. Thus, the power of the reformate (kW) would be expected to be greater when the CO and unburnt hydrocarbons (already present in the engine exhaust gas) are taken into account.

At around 700°C, equilibrium calculations show that the reforming reactions should be approaching their optimum (as can be seen from the product gas composition in **Figure 3**), so the actual improvements in the heating value are expected to be close to the maximum theoretical value of 27% for stoichiometric reaction. At lower exhaust gas temperatures, the process efficiency will be reduced and could even be <100%, as complete oxidation of part of the fuel is likely. The process efficiencies predicted for the different temperatures, based on the equilibrium model are shown in **Figure 5**, together with the predictions from the stoichiometric model.

The maximum process efficiency from the equilibrium model (120%) is lower than the efficiency calculated under stoichiometric conditions (127%). This difference is mainly due to the equilibrium model predicting incomplete conversion of CO_2 and H_2O over the complete temperature range, whereas the stoichiometric model assumes that they are completely consumed through dry- and steam-reforming reactions, respectively.

The stoichiometric model predicted the fuel saving for System 1 to be 21.4% at all the operating points considered in this study, whereas the equilibrium model predicted values over the range 11–14% (**Figure 6**). Not surprisingly, predicted fuel savings for System 2 were consistently lower (**Figure 7**), with the stoichiometric model predicting 12.1%, whereas the equilibrium model gave an average of 6.5% over the range of operating points.

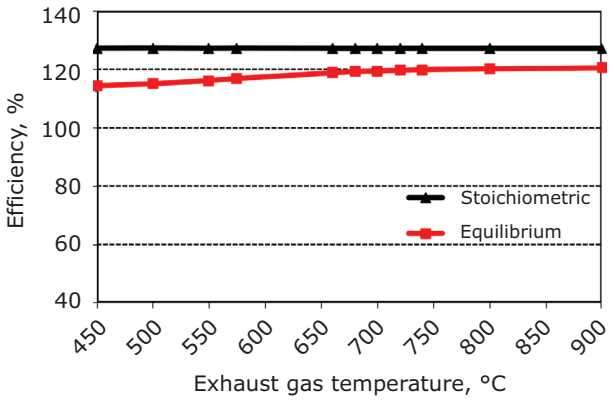

Fig. 5. Comparison of process efficiencies based on the stoichiometric and equilibrium calculations

Part II: Experimental Testing

Reformer Output

When the small-scale exhaust gas reformer was tested under the conditions shown in **Table III**, the changes in outlet concentrations of CO, H_2 and CO_2 as a function of temperature (**Figure 8**) followed the trends predicted by the equilibrium models. However, there was a persistent low THC concentration (600–1000 ppm) indicating the presence of unconverted hydrocarbons at all temperatures. These unconverted hydrocarbons are most likely to be the endothermic thermal cracking products formed from the higher hydrocarbons in the gasoline. Further mechanistic insights come from the changes in relative proportions of the products. The CO-concentration trace rises sharply between 600°C and 800°C, resulting in two almost linear regimes with different gradients. However, the gradient of the H_2-concentration trace does not change over the entire temperature range studied. As a result,

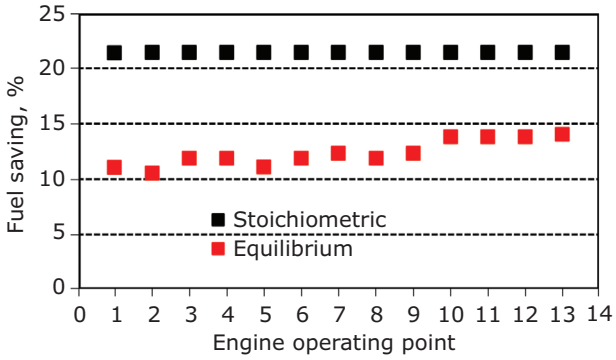

Fig. 6. Predicted fuel savings for System 1 under the different engines assessed, based on the two models

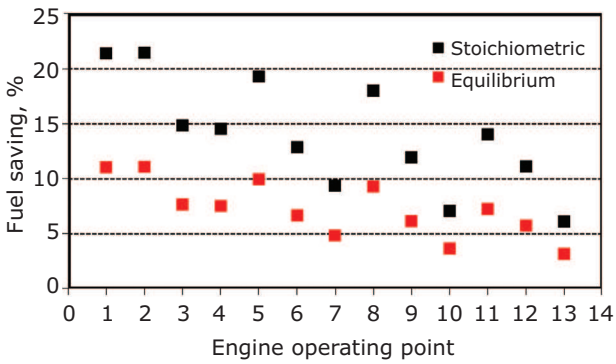

Fig. 7. Predicted fuel savings for System 2 under the different engines assessed, based on the two models

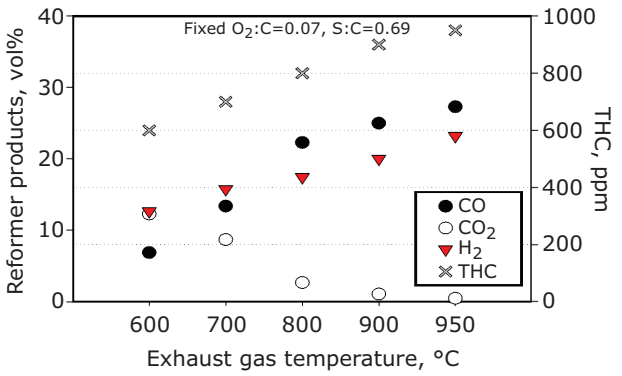

Fig. 8. Output of exhaust gas reformer as a function of exhaust gas temperature

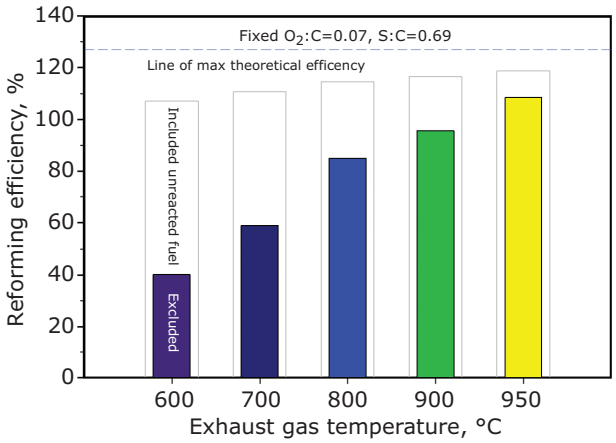

Fig. 9. Efficiency of exhaust gas reformer as a function of temperature

two distinctive H_2:CO ratios of 1.84 and 0.83 are observed for the product stream, with a break-point in between at around 750°C. These values show 90–95% agreement with the stoichiometric H_2:CO ratios for wet- and dry-reforming of 1.92 and 0.92 respectively, suggesting that the reforming process was dominated by the gasoline+steam reaction at exhaust gas temperature regimes below 750°C, before the gasoline+CO_2 reaction predominated. Perhaps significantly, in an earlier study of exhaust gas reforming of ethanol using a rhodium-containing catalyst system (17), we observed a similar transition from steam- to dry-reforming at around 750°C.

Process Efficiency

To convert the performance measurements (in **Figure 8**) into working efficiencies, we compared the heating value of the product stream exiting the exhaust gas reformer with the heating value of the gasoline being fed to it. In one set of calculations, we took into account only the CO and H_2 formed; while in another we also included the unconverted (cracked) hydrocarbons in the product stream. The results of both sets of calculations are presented in **Figure 9**, showing the general trend of higher exhaust temperature resulting in higher reforming efficiency.

In a real operating system, the exhaust gas reformer will be close-coupled with the engine (12, 18). This means that all the components of the reformer product-stream will be fed directly into the engine. Therefore, in calculating the predicted fuel savings, we have used the higher efficiency values (from 107% at 600°C, to 119% at 950°C), which included the THC content of the product stream. From these calculations we estimate that, if 50% of the gasoline fuel is being reformed (and the reformer products are fed to the engine), then the potential fuel saving will be between 3.6% and 9.4% depending on the exhaust gas temperature (**Figure 10**). Additional calculations have shown that the maximum value could be increased to 10.5%, with water addition to the exhaust gas reformer.

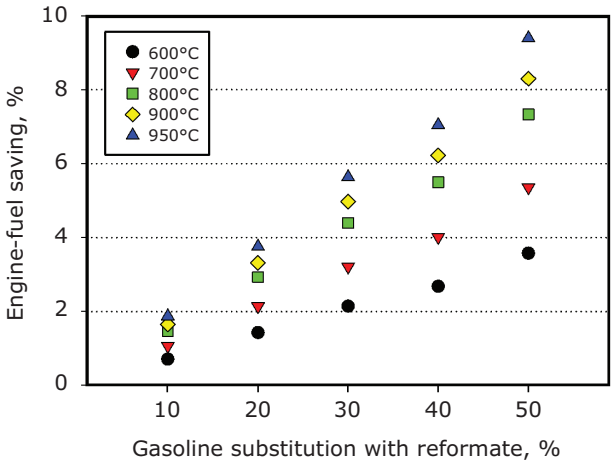

Fig. 10. Effect on predicted overall fuel savings achieved through fuel-by-reformate substitution in a gasoline engine, over a range of exhaust gas temperatures

Conclusions

Based on a thermodynamic model, which assumes that an exhaust gas reformer can achieve chemical

equilibrium under gasoline exhaust gas conditions, we have calculated an expected fuel saving of 4–14% for a close-coupled engine+reformer system. From analysis of the reformate produced by a highly active catalyst fed with real exhaust gas (to which gasoline was added), we consider that a more realistic range is 3.6–9.4%, with these differences mainly due to kinetic, enthalpy and mass-transfer limitations. The top end of this range slightly exceeds the maximum of 8.3% predicted by Szybist and co-workers (18) in a closely related but independent study, which investigated a similar range of catalyst inlet compositions, temperatures and residence times, though using a catalyst with a higher loading of rhodium. However, both values are likely to be underestimates, as close-coupled reforming requires a wider throttle opening position, in order to maintain combustion stoichiometry inside the engine. The widened throttle will result in reduced engine-pumping loss (19), which is likely to contribute an additional fuel saving of approximately 1–2% (20). These results suggest that the high fuel economy and low CO_2 release associated with diesel vehicles could be matched by a gasoline SI vehicle fitted with an exhaust gas reformer. Furthermore, a gasoline vehicle fitted with this technology would still only require a three-way catalytic converter to ensure that its emission quality (as measured by the rate of release of local pollutants – NOx, hydrocarbons, CO, particulate) exceeded that of current diesel vehicles.

Aknowledgements

All the authors thank the EPSRC for funding the work described, which was part of the project 'Clean Low Carbon Vehicles – Combustion with Simultaneous Nitrogen and Hydrogen Enrichment' (EP/H050248/1); P. Leung also thanks the University of Birmingham for the award of a PhD scholarship.

References

1. "Climate Change 2014: Mitigation of Climate Change", eds. O. Edenhofer, R. Pichs-Madruga, Y. Sokona, J. C. Minx, E. Farahani, S. Kadner, K. Seyboth, A. Adler, I. Baum, S. Brunner, P. Eickemeier, B. Kriemann, J. Savolainen, S. Schlömer, C. von Stechow and T. Zwickel, Intergovernmental Panel on Climate Change (IPCC), Geneva, Switzerland, 2014, 1454 pp
2. M. Lapuerta, J. Rodriguez-Fernandez and J. M. Herreros, 'Gaseous and Particle Greenhouse Emissions from Road Transport', in "Environmental Impacts of Road Vehicles: Past, Present and Future", eds. R. M. Harrison and R. E. Hester, The Royal Society of Chemistry, London, UK, 2017, pp. 25–45
3. C. Sprouse III and C. Depcik, *Appl. Therm. Eng*., 2013, **51**, (1–2), 711
4. C. O. Katsanos, D. T. Hountalas and T. C. Zannis, *Energy Conv. Manage*., 2013, **76**, 712
5. D. H. Lee, J. S. Lee and J. S. Park, *Appl. Energy*, 2010, **87**, (5), 1716
6. X. Liang, X. Wang, G. Shu, H. Wei, H. Tian and X. Wang, *Int. J. Engine Res*., 2015, **39**, (4), 453
7. D. Fennell, J. Herreros, A. Tsolakis, K. Cockle, J. Pignon and P. Millington, *RSC Adv*., 2015, **5**, (44), 35252
8. M. Bogarra, J. M. Herreros, A. Tsolakis, A. P. E. York and P. J. Millington, *Appl. Energy*, 2016, **180**, 245
9. J. Barbier Jr. and D. Duprez, *Appl. Catal. B: Environ*., 1994, **4**, (2–3), 105
10. J. W. Jenkins and E. Shutt, *Platinum Metals Rev*., 1989, **33**, (3), 118
11. N. Edwards, S. R. Ellis, J. C. Frost, S. E. Golunski, A. N. J. van Keulen, N. G. Lindewald and J. G. Reinkingh, *J. Power Sources*, 1998, **71**, (1–2), 123
12. K. Geissler, E. Newson, F. Vogel, T.-B. Truong, P. Hottinger and A. Wokaun, *Phys. Chem. Chem. Phys*., 2001, **3**, (3), 289
13. S. Golunski, *Platinum Metals Rev*., 1998, **42**, (1), 2
14. S. Golunski, *Energy Environ. Sci*., 2010, **3**, (12), 1918
15. C. S. Lau, D. Allen, A. Tsolakis, S. E. Golunski and M. L. Wyszynski, *Biomass Bioenergy*, 2012, **40**, 86
16. E. D. Sall, D. A. Morgenstern, J. P. Fornango, J. W. Taylor, N. Chomic and J. Wheeler, *Energy Fuels*, 2013, **27**, (9), 5579
17. S. Peucheret, M. Feaviour and S. Golunski, *Appl. Catal. B: Environ*., 2006, **65**, (3–4), 201
18. Y. Chang, J. P. Szybist, J. A. Pihl and D. W. Brookshear, *Energy Fuels*, 2018, **32**, (2), 2245
19. P. Leung, A. Tsolakis, J. Rodríguez-Fernández and S. Golunski, *Energy Environ. Sci*., 2010, **3**, (6), 780
20. Y. Chang, J. P. Szybist, J. A. Pihl and D. W. Brookshear, *Energy Fuels*, 2018, **32**, (2), 2257
21. J. B. Heywood, 'Engine Friction and Lubrication: Engine Friction Data: SI Engines', in "Internal Combustion Engines Fundamentals", McGraw-Hill Inc, New York, USA, 1988, pp. 722–723
22. D. A. Fennell, 'Exhaust Gas Fuel Reforming for Improved Gasoline Direct Injection Engine Efficiency and Emissions', PhD thesis, University of Birmingham, Birmingham, UK, 2014

The Authors

Perry Leung obtained his PhD from the University of Birmingham, UK. He was then employed as diesel engine calibration and development engineer with Perkins Engines 2013, project engineer at FEV GmbH 2017 and Ricardo 2018. He is the CEO/Co-Founder of MEEG, Aachen, Germany.

Professor Athanasios Tsolakis has academic and industrial expertise in the field of low carbon energy carriers, environmental catalysts, combustion and pollutant control technologies. Prior to his academic appointment at the University of Birmingham in 2005 he worked as a research scientist at Johnson Matthey in the design and characterisation of environmental catalysts for aftertreatment systems. Since 2015 he is the Director of Research for the School of Engineering at the University of Birmingham.

Jose M. Herreros is a Lecturer at the School of Engineering at the University of Birmingham. His research focuses on the investigation of clean and efficient powertrain systems based on the energy and emissions efficient integration of various propulsion systems with the ultimate goal to develop energy-efficient and clean powertrains to be used in vehicular applications. He has published journal articles on issues related to fuel design and properties, pollutant emissions characterisation and catalysis.

Miroslaw L. Wyszynski joined the University of Birmingham from Warsaw University of Technology, Poland, and used his expertise on the border of mechanical and chemical engineering to create research activity in on-board fuel reforming with exhaust gas from internal combustion engines.

Stan Golunski began his research career in industry, before becoming Professor of Catalysis and later Co-Director of the Cardiff Catalysis Institute at Cardiff University, UK, until July 2018. His research interests lie in the fundamentals and applications of supported nanoparticle catalysts, mainly in the context of water and air purification for environmental protection.